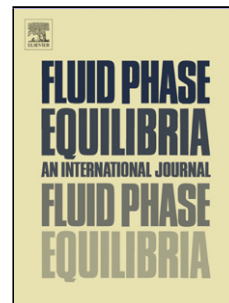


Accepted Manuscript

Title: Hydrophobicity and geometry: water at curved graphitic-like surfaces and within model pores in self-assembled monolayers

Author: L.M. Alarcón J.M. Montes de Oca S.R. Accordino
J.A. Rodríguez Fris G.A. Appignanesi



PII: S0378-3812(13)00503-7
DOI: <http://dx.doi.org/doi:10.1016/j.fluid.2013.09.008>
Reference: FLUID 9756

To appear in: *Fluid Phase Equilibria*

Received date: 14-7-2013
Revised date: 4-9-2013
Accepted date: 5-9-2013

Please cite this article as: L.M. Alarcón, J.M. Montes de Oca, S.R. Accordino, J.A. Rodríguez Fris, G.A. Appignanesi, Hydrophobicity and geometry: water at curved graphitic-like surfaces and within model pores in self-assembled monolayers, *Fluid Phase Equilibria* (2013), <http://dx.doi.org/10.1016/j.fluid.2013.09.008>

This is a PDF file of an unedited manuscript that has been accepted for publication. As a service to our customers we are providing this early version of the manuscript. The manuscript will undergo copyediting, typesetting, and review of the resulting proof before it is published in its final form. Please note that during the production process errors may be discovered which could affect the content, and all legal disclaimers that apply to the journal pertain.

Hydrophobicity and geometry: water at curved graphitic-like surfaces and within model pores in self-assembled monolayers

L. M. Alarcón¹, J. M. Montes de Oca, S. R. Accordino², J. A. Rodríguez Fris and G. A. Appignanesi

Sección Fisicoquímica, INQUISUR-UNS-CONICET and Departamento de Química, Universidad Nacional del Sur, Avenida Alem 1253, 8000-Bahía Blanca, Argentina.

¹ lalarcon@uns.edu.ar, ²sebastian.accordino@uns.edu.ar

Abstract

In this work we perform molecular dynamics simulations of water in contact with simple model hydrophobic surfaces and pores in order to test the role of local geometry on hydrophobicity. Specifically, we study different quantities like orientational ordering, density fluctuations and water residence times (autocorrelation functions) around graphene sheets, at the exterior of single-walled carbon nanotubes, at alkane-like self-assembled monolayers (SAMs) and at pores of different sizes carved in such SAMs. We show that in the case of the convex graphitic-like surfaces, the curvature does not affect the local hydrophobicity. However, a significant curvature dependence will be made evident for the concave surfaces of the pores carved in the SAMs. The geometrically-induced dehydration that occurs as the pore size reaches the subnanometric regime might be operative in realistic settings like protein binding sites which require water removal upon ligand binding.

Keywords:

hydrophobicity, water, graphene, carbon nanotubes, self assembled monolayers

1. Introduction

A complete knowledge of the behavior of water at interfaces and under nanoconfinement is expected to open new roads of both academic and technological relevance in fields ranging from biology to materials science

[1, 2, 3, 4, 5, 6, 7, 8, 9, 10, 11, 12]. Both in biological organization and in the supramolecular self-assembly of materials, the nanoconfinement that arises upon the interaction of the different assembling units affects the thermodynamic properties of the hydration water, which usually must be removed for the process to take place[7]. In such contexts, bulk-like knowledge could be not only useless but also misleading and a new intuition and new principles become necessary towards a molecular-scale theory of hydrophobicity. Thus, it is not surprising that today rational design is practically absent in contexts ranging from drug design to the design of soluble self-assembled materials. Most of the non-covalent interactions (mainly the ones which are electrostatic in nature) invoked in such fields would not be operative in bulk water conditions. However, the different non-covalent interactions (like hydrogen bonds, ionic interactions and hydrophobic interactions) can be clearly non-additive under nanoconfinement, a context-dependent nature which is usually overlooked in design efforts.

In realistic contexts, both chemistry and local geometry are expected to define the local hydrophobicity[7]. In particular, the hydration properties of protein binding sites have been suggested to play a main role in the binding of ligands or in protein-protein association[9, 11, 13]. From one side, ligands are expected to displace hydration water molecules from their binding site[9, 13]. On the other hand, geometrically-induced surface dehydration (by means of water inaccessible cavities) has been shown to be central for the existence of reactive sites responsible for protein binding[11, 13]. In addition, the behavior of water confined in cylindrical pores or tunnels is also important both from the basic and the applied viewpoints. For instance, this behavior is relevant for water flow in aquaporins and proton flow in proton pumps and enzymes[8]. While it is generally believed that small protein cavities are empty[9], there is no general consensus on whether large protein cavities are filled or empty and certain experimental results on the subject are contradictory (even when certain large cavities seem to indeed present small clusters of confined water molecules)[9, 8]. In turn, it has been shown that subnanometric nonpolar cavities (spherical pores) remain empty, whereas water penetrates nanometric size ones[8, 14, 15]. This behavior is due to the reluctance of the water molecules to resign hydrogen bond coordination with other water molecules (only nanometric size cavities allow penetration retaining the coordination typical at surfaces). For example, the interiors of the spherical C_{180} and C_{140} fullerenes (the size of the last one being barely larger than 10\AA) have been shown to present stability for filled states with

small clusters of water molecules connected by strong hydrogen bonds[8, 14]. Additionally, the filling and the conduction of water in carbon nanotubes and related systems has been extensively studied[8, 16, 17, 18, 19, 20, 21?] and many different water phases have been discovered (from 1D trains of hydrogen-bonded water molecules at low nanotube radius to complex layered structures within larger nanotubes[8, 16, 17, 18]). It has also been shown that the hydrophobicity of the material is important since a small reduction of the van der Waals attraction between water and the carbon atoms induces the drying of previously filled nanotubes[8]. Additionally, it has been shown that the minimum radius of a tunnel carved in hydrophobic self-assembled monolayers that gets wet is roughly twice as large as the radius of the smaller carbon nanotube that gets filled.

While different structural, dynamical and thermodynamical measures of hydrophobicity have been proposed[23], a very interesting one consists in the quantification of water density fluctuations[23]. It has been demonstrated that superficial water density profiles do not represent a good measure of surface hydrophobicity. This can be expected in terms of the usual knowledge that water abhors vacuum and thus, water molecules tend to hydrate both polar and nonpolar surfaces and the normal density profiles display similar characteristics, with layering structure, in both cases. However, at variance from hydrophilic surfaces where the water molecules are subject to significant attractive interactions, at hydrophobic surfaces the interactions are very weak, which makes the hydrating water molecules to display low residence times and to become easily removed. Thus, such hydration layers display enhanced dynamics[23], enhanced compressibility[23, 7] and enhanced density fluctuations[23]. In particular, the density fluctuations at differently functionalized self-assembled monolayers (SAMs) have been characterized demonstrating that hydrophobic-like surfaces do in fact present much larger density fluctuations than the ones displayed by hydrophilic-like surfaces, thus providing a good quantitative measure of hydrophobicity. Normalized fluctuations of water number density, $\sigma_N^2 / \langle N \rangle^2$ in small observation volumes (where N is the number of water molecules within such volume) are approximately equal to $2\mu^{ex}/kT$, where μ^{ex} is the free energy of formation of cavity of such radius[24]. Thus, a high value of the normalized density fluctuations at a given place indicates a favorable work of cavity creation at such place[24] and, thus, a high hydrophobicity.

Within this context, the aim of the present work is to explore, by means of molecular dynamics simulations, the behavior of water in contact with

simple model hydrophobic surfaces and pores so as to shed some light on the role of the local geometry on hydrophobicity. In complex systems (like protein hydration for example), both local chemistry and curvature affect the local hydrophobicity and it is usually difficult to disentangle both effects. Curvature is expected to play a main role since, as already indicated above protein cavities show a propensity to dehydration. Thus, the study of model settings that separate the effect of geometry from that of chemistry is of interest. Our work provides one such study where chemically simple systems with different curvatures (both concave and convex) are used so as to quantify the effect of geometry. Thus, we shall study different hydrophobicity measures like orientational ordering, density fluctuations and dynamic quantities around graphene sheets, at the exterior of single-walled carbon nanotubes, at alkane-like SAMs and at pores of different sizes carved on such SAMs. For the convex surfaces of carbon nanotubes, we shall show that the effect of curvature on hydrophobicity is almost negligible. However, we shall show the significant role of geometry in increasing hydrophobicity and even in promoting dehydration as the size of the pore is reduced towards the subnanometric size in the SAMs.

2. Methodology

From one side, we studied a graphene sheet and single walled carbon nanotubes of different radii. Given the chemical similarity between such systems, the hydration of the graphene sheet should constitute the limit of infinite curvature radius for the nanotubes. The water molecules were modeled by the TIP3P model[25, 26]. The equilibration of the whole system was carried out in two parts: In the first one we used a Berendsen thermostat [27] within the canonical NVE ensemble, and in the second part of the equilibration we used a NPT ensemble with a Langevin thermostat[28]. The production runs and calculations were performed in the NPT ensemble with a Langevin thermostat. All simulations were done using the AMBER10 molecular simulation suite[29] with a 1 fs time step (we used the GAFF and FF99SB force fields for carbon and water, respectively). All calculations were performed in the NPT ensemble with a Langevin thermostat. The model graphene surface was a perfect honeycomb graphite-like sheet, consisting of a layer of 20 by 20 benzenic rings (approximately 2300\AA^2) with terminations in hydrogen atoms solvated with 11,644 TIP3P water molecules in an orthogonal cubic box with periodic boundaries[10]. The surface was centered in the middle of the box

and parallel to the XY plane. The water molecules studied were located more than 2 Å away from the borders of the graphene sheet. In turn, the carbon nanotubes employed were single walled carbon nanotubes with a zig-zag arrangement and one of them had a radius of 2.0 Å while the other had a radius of 28 Å. Each of the nanotubes was solvated in a box of TIP3P water molecules that extended more than 20 Å away from the nanotube borders in each direction. The axis of the nanotube coincided with the x axis and the length of the nanotubes was 14 Å in all cases and thus, this dimension was always extensive. In all cases, the regions studied were more than 2 Å apart from the nanotube x-endings in order to avoid border effects. In this work we shall consider only the exterior, convex, surface of the nanotube.

For the hydrophobic pores we constructed monolayers of 81 chains (9×9) and monolayers of 144 chains (12×12) of n-decane ($CH_3 - (CH_2)_8 - CH_3$) aligned in a parallel fashion so as to generate a cube. This arrangement mimics the monolayer structure of stearic acid chains adopted at a water interface but replaces the acid group (COOH) by a H so that the chain ends with a methyl, ie. it becomes a n-decane chain. In this case, the SAM system constitutes just a model hydrophobic setting to focus on the behavior of the surrounding water. The original chain separation was 4.53 Å, the typical distance in a fatty acid monolayer. Our alkane-like chains were built parallel to each other and placed in a square arrangement, that is, with the heads of the chains arranged in a square (we mention that we also studied some hexagonal arrangements and found similar results). Each monolayer was solvated with water molecules modeled by the TIP3P model[25, 26] in an orthogonal cubic box with periodic boundary conditions and was equilibrated within a canonical NVE ensemble with a Berendsen thermostat [27]. The size of the box was such that it extended more than 20 Å away from all the monolayer faces. The surface monolayer was centered in the middle of the box. All simulations were done using the AMBER10 molecular simulation suite[29] with a 2 fs time step (we used the GAFF and FF99SB force fields) and all calculations were performed in the NPT ensemble with a Langevin thermostat. The monolayer without a hole will be called “perfect” monolayer from now on. For the cavities, we carved holes in the monolayer surface parallel to the (x,y) plane in the z direction (the positions of the hydrogens at the top of the monolayer was $z = 42.5$ Å while the corresponding carbon atoms were placed at $z = 41.6$ Å. In all cases (perfect monolayer or with the different carved holes) the AMBER equilibration reduced the distance between the n-decane molecules (the chain separation) to 4.2 Å. To generate

the cavities we carved squared holes of different sizes at the center of the monolayer surface by cutting the corresponding number of chains (the bonds of the carbon atoms at the bottom of the hole were saturated so that all chains ended with a methyl group; in other words, they became shorter chain alkanes). For the holes we shall use the following nomenclature: $A \times B$ means that the chains of a number A of molecules conforming a square at the center of the monolayer were shortened in B units (the depth of the hole is thus given by $B \times 1.2\text{\AA}$ where 1.2\AA is the length of a CH_2 monomer). We studied 1×5 , 4×5 , 9×5 , 16×5 , 25×5 , 36×5 , 49×5 and 64×5 , together with the perfect monolayer. All the holes were carved at the center of the monolayer face, so that they were always far enough from the borders of the monolayer. For holes of size up to 25×5 we used the (9×9) and monolayers, while for the larger three holes we used the larger (12×12) and monolayers. Table 1 summarizes the different holes carved in the monolayers.

SAM	Hole width [\AA]	Hole depth [\AA]
1x5	8.5	6.4
4x5	12.7	6.4
9x5	16.5	6.4
16x5	21.3	6.4
25x5	25.1	6.4
36x5	29.5	6.4
49x5	33.8	6.4
64x5	38.0	6.4

Table 1: We summarize the different holes carved in the SAMs, indicating the width and depth of the holes. The pore depth is measured between C atoms at the same height at opposite walls of the pore. As all the holes were produced by shortening the corresponding number of chains in 5 units, all depths are equal.

For all studied systems we carried simulations at a temperature of $T = 300K$ (however, in certain cases we employed a lower temperature $T = 240K$, as shall be explicitly pointed out), mean pressure of 1 bar and average density around 1.0 kg/dm^3 . We used a short range interaction cutoff of 8\AA with particle mesh Ewald[30]. Equilibration was tested by monitoring the behavior of thermodynamical properties like temperature, pressure and energy oscillations, and by dynamical properties like oscillations in the mean squared displacement of the water molecules; the equilibration times were in each case far much larger than the structural relaxation time, τ_α , for pure water

at this temperature (τ_α is the timescale when the self-intermediate scattering function evaluated at the first peak of the structure factor has decayed to $1/e$).

3. Results and discussion

Previous works have determined that water molecules around graphitic-like surfaces (within the first layers of the normal density plot) display a preferential orientational ordering resembling the structure of hexagonal ice (ice Ih)[10, 31, 32]. Thus, the water molecules closest to the surface sacrifice the lowest hydrogen bond (HB) coordination by orienting a vertex of the tetrahedron towards the surface, but contrary to the water-air[32, 33] or water-vacuum[34] interfaces, they do not orient an H atom towards the surface but an electron lone pair[10, 31]. Thus, they lose one hydrogen-bond coordination water partner due to the presence of the surface. In Fig. 1 we present the orientational ordering of the water molecules within the first peak of the density plot for graphene, a small radius carbon nanotube and the alkane-like SAM without hole. We plot the probability of $\cos(\theta)$, where θ is the angle formed by the OH bonds of the water molecules with the normal to the surface. This quantity is interesting since it is amenable of comparison with experimental surface sum-frequency vibrational spectroscopy data[32], when available. From such a figure we can learn that the molecules close to the graphitic surfaces have clear preferential ordering, at variance from the situation for bulk water (water molecules far from the surfaces display small fluctuations around a flat horizontal line in all cases). The distributions for such water molecules close to the surface show a peak corresponding to angles of 70° , that is, they tend to orient with a vertex of the tetrahedron (an electron lone pair), an orientation consistent with that of the basal plane of ice Ih[32, 10, 31]. Such orientational tendency changes little when we go from the graphene sheet to a low radius carbon nanotube, which speaks of the fact that the a change in curvature for these convex surfaces does not produce significant alterations in the orientational ordering of the hydrating molecules. In turn, when we now study the behavior of water molecules over the hydrophobic SAM, we learn that they also display a clear preferential orientational tendency. However, such molecules display an angle between $100^\circ - 110^\circ$, and thus tend to orient a face of the tetrahedron parallel to the SAM surface.

We have also calculated the angle between the dipoles of the water molecules

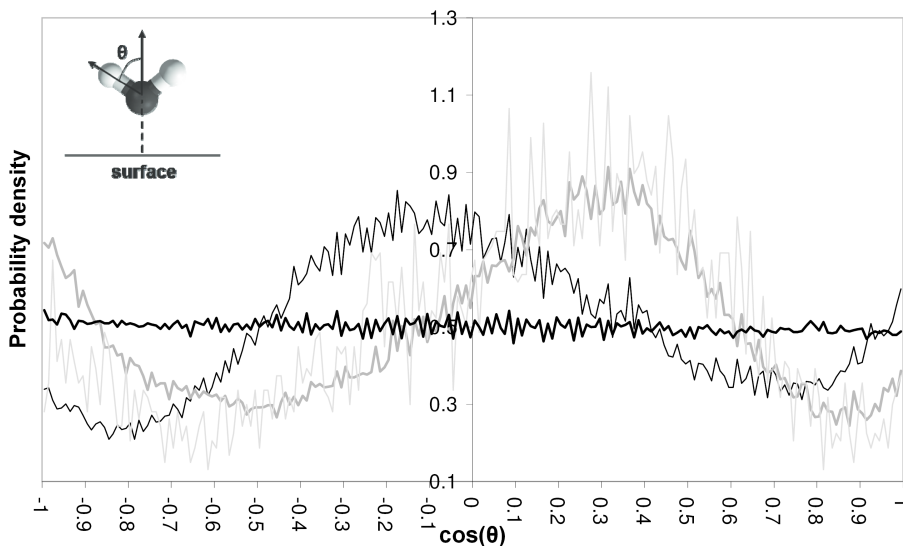


Figure 1: Distribution of $\cos\theta$ for water molecules close to the graphene surface (light gray curve), the carbon nanotube of radius 2.0 \AA (dark gray), the alkane-like SAM without hole (thin black line) and for bulk water (thick black line), that is, for water far from the graphene surface (identical results are obtained for water far from the other surfaces). In this case we reduced temperature to $T = 240K$ to get neater peaks, but similar results were obtained for $T = 300K$. For graphene and the SAM, θ is the angle between the OH bond of the water molecule and the normal to the surface, while for the carbon nanotube it is measured with respect to the line perpendicular to the nanotube axis that passes through the oxygen atom of the corresponding molecule. We also include an inset to better illustrate the angle calculated.

and the surface normal, which we call θ_{dp} . In Fig. 2 we show the distribution of this quantity for the case of the perfect SAM and for the graphene sheet (results for the carbon nanotubes are similar to that for graphene). These results are consistent with the previous analysis based on the OH angle. In both cases we find preferential ordering (with a better ordering in the case of graphene) and in both cases there is a tendency for the plane H-O-H (the plane that contains the dipole vector) to be oriented almost parallel to the surface.

In a different trend, previous results obtained by calculating the local structural index [10, 35, 36] have shown that the water molecules close to a graphene surface are well (tetrahedrally) structured and that such structuring is similar for water molecules at the exterior wall of large radius carbon

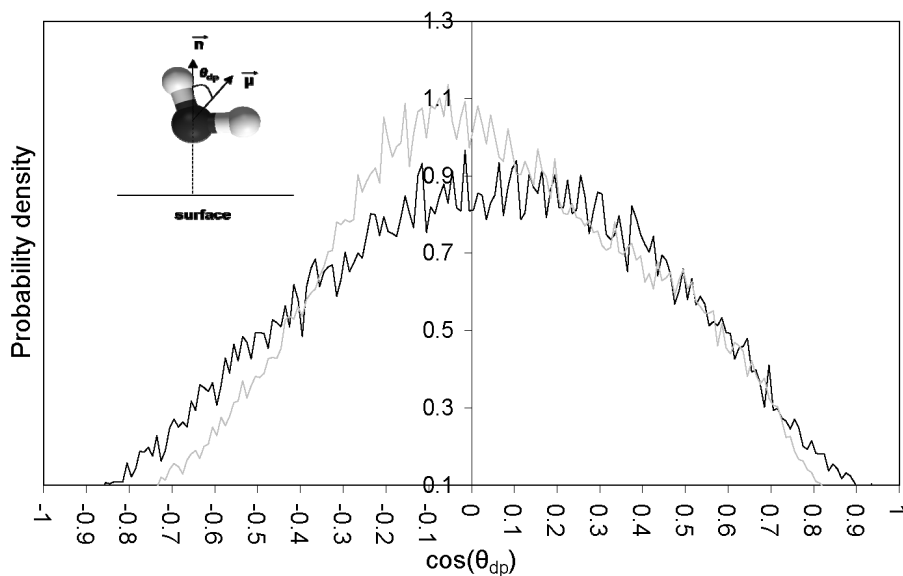


Figure 2: Distribution of the cosine of the angle θ_{dp} formed between the dipole vector of the water molecule and the normal to the surface. We show the cases for the water molecules close to the graphene surface (light gray curve) and to the alkane-like SAM without hole (thin black line).

nanotubes. However, when we consider nanotubes with radii within the sub-nanometric range, a significant loss in the structuring of the exterior water is observed. Thus, we are interested in determining whether the geometrically-induced destructuring of hydration water is coupled to hydrophobicity effects. In Fig. 3 we display the probability distributions for observing N water molecules, $p(N)$, within a small spherical observation volume of radius 3.3\AA (similar to a methane molecule) tangent to the different graphitic-like surfaces studied (results correspond to graphene and to carbon nanotubes of radius 2 and 28\AA). The wider the distribution, the greater the water density fluctuations at such location. From such figure, we can learn that the water density fluctuations, and thus, the hydrophobicity of the surface, does not depend appreciably on curvature.

Another quantity that should reflect the degree of surface hydrophobicity are water residence times. Residence times are expected to decrease with increasing the hydrophobicity of the surface (while they would be large over hydrophilic surfaces). Thus, we calculated water residence times within the spheres tangent to the surfaces by means of a water autocorrelation func-

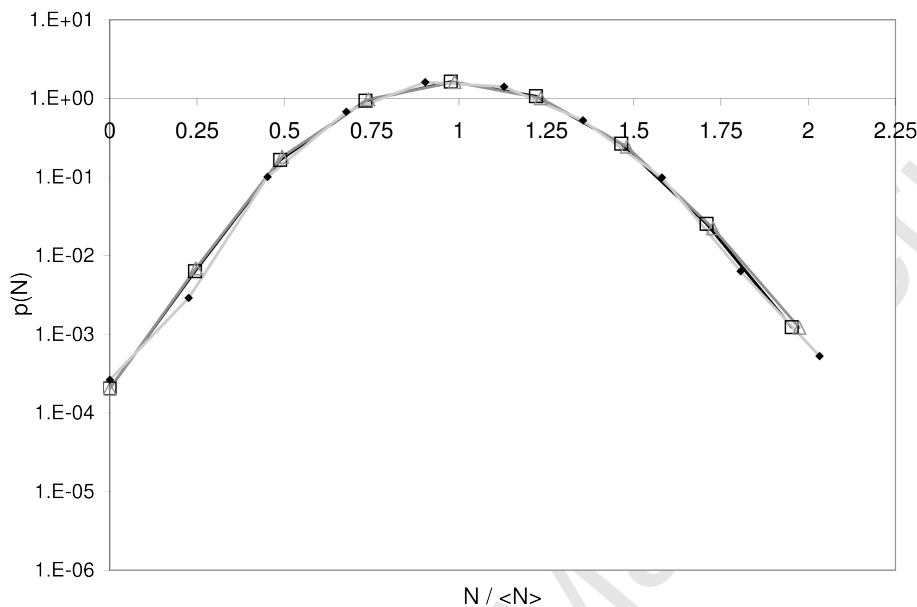


Figure 3: Probability distribution $p(N)$ for the graphene sheet (squares) and for carbon nanotubes of radius 2 Å (triangles) and 28 Å (filled small diamonds)

tion. Such autocorrelation function is defined as $C(t) = \langle R(0)R(t) \rangle / \langle R(0) \rangle^2$, where $R(t)$ is a residence function defined by $R(t) = \sum_i R_i(t)$, where the index i runs over all the molecules i that at time $t = 0$ were placed within the sphere. $R_i(t)$ is 1 whenever the i water molecule is within the sphere while it becomes 0 otherwise. Fig. 4 shows the water autocorrelation function for spheres of radius 3.0 Å tangent to the graphene sheet and to the different nanotubes. Again, this figure tells us that for such convex surfaces hydrophobicity does not depend appreciably on curvature and reinforces the notion that water density fluctuations represent good measures of hydrophobicity.

To study the effect of concavity on hydrophobicity, we carved several cavities on the hydrophobic SAMs. This geometrical setting is of particular interest given the situations found in protein pockets and in pores at different materials. We calculated the normalized density fluctuations, $\sigma_N^2 / \langle N \rangle^2$, of the probability distributions for observing N water molecules within spheres located at the “mouth” of the different holes 1×5 , 4×5 , 9×5 , 16×5 , 25×5 , 36×5 , 49×5 and 64×5 . This means that the observation spheres were

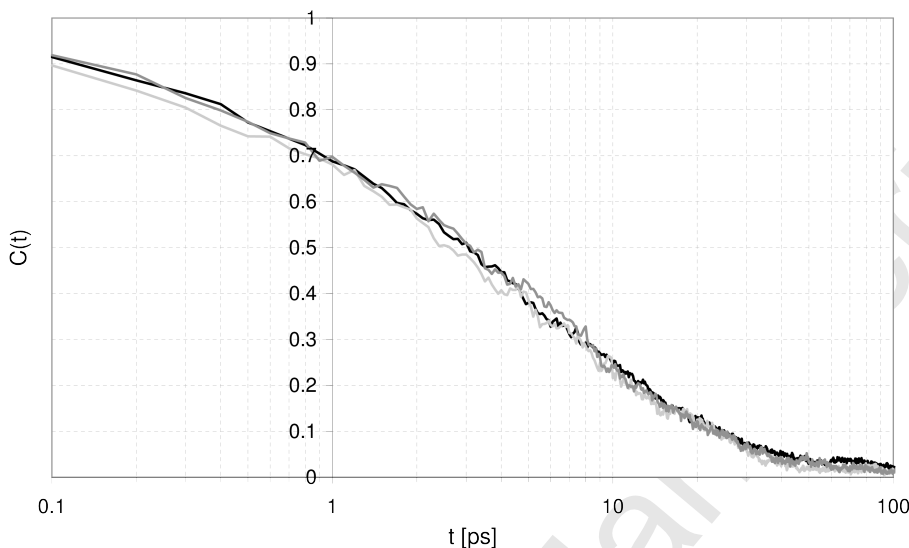


Figure 4: Water autocorrelation function, $C(t)$, for graphene (black line) and for carbon nanotubes of radius 2 Å (light gray) and 28 Å (dark gray)

located inside the hole, almost tangent to the line defined by the H atoms of the methyls of the alkylic chains framing the holes ($z = 42.5$ Å). Additionally, all spheres were also placed at the center of the corresponding segment that defines the top of each hole. In Fig. 5 and Fig. 6 we sketch the 1×5 and 25×5 holes, respectively.

Fig. 7 depicts the density fluctuations for the different holes. We also include the situation for the perfect monolayer (without hole), where the sphere is located tangent to the surface. From such figure we can learn that the degree of hydrophobicity strongly depends on curvature. The holes are more hydrophobic than the perfect monolayer, but the role of geometry is more conspicuous as the hole size (the diameter of the hole “mouth”, L) approaches the subnanometric regime (as evident from Fig. 7 Right). Such subnanometric-sized holes do not fill with water given the reluctance of the water molecules to lose their hydrogen bond coordination in order to penetrate. Larger holes (up to roughly $L = 25$ Å), where the water molecules can enter retaining their coordination, are nonetheless more hydrophobic than the perfect monolayer, which means that hydrophobicity is clearly curvature-dependent for concave surfaces. Such result of a geometrically-induced dehydration is interesting, for example, for the context of protein binding, since

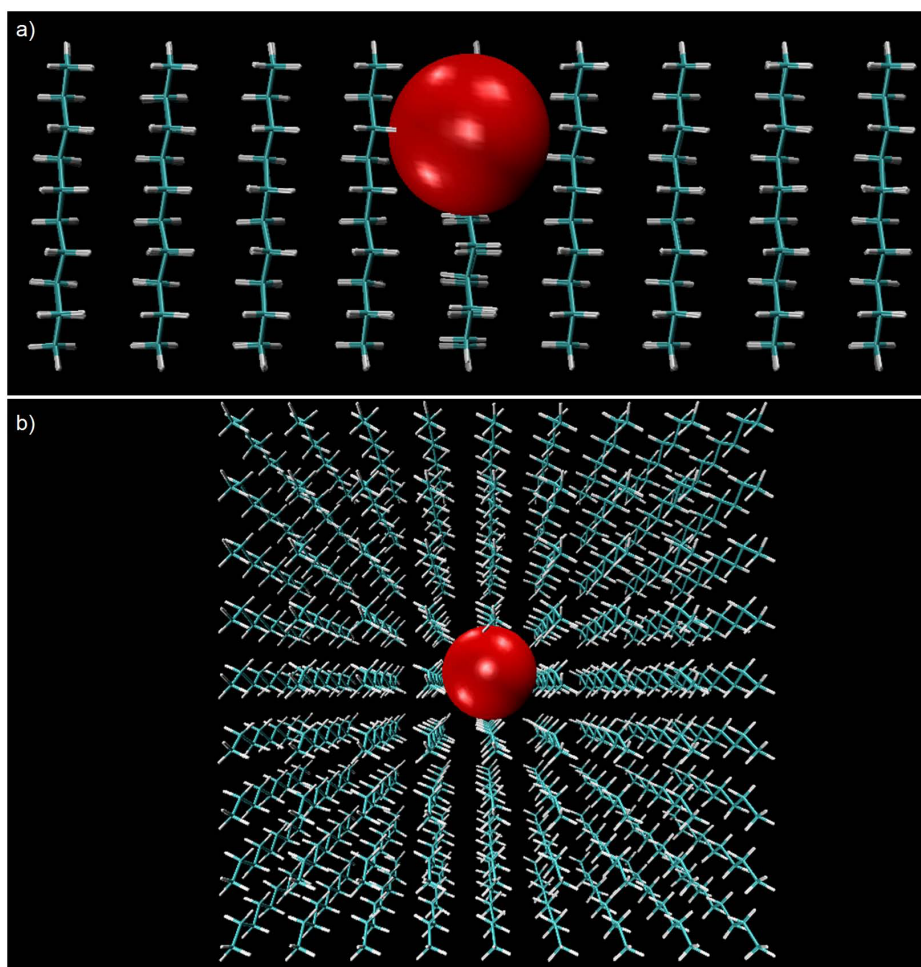


Figure 5: Illustration of the SAM with a hole 1×5 . The nomenclature $A \times B$ means that the chains of a number A of molecules conforming a square at the center of the monolayer were shortened in B units. Here it indicates that one chain (the central alkane chain) has been shortened in 5 units to create the pore. a) We show a side view of the alkane-like monolayer, which we have cut at the middle in order to better display the hole. The red sphere indicates the observation volume used. b) Top view of the monolayer. Table 1 summarizes the different holes we carved in the monolayers.

protein binding pockets are expected to be dry or to contain easily removable water which should be displaced by a ligand upon association[9, 2, 13].

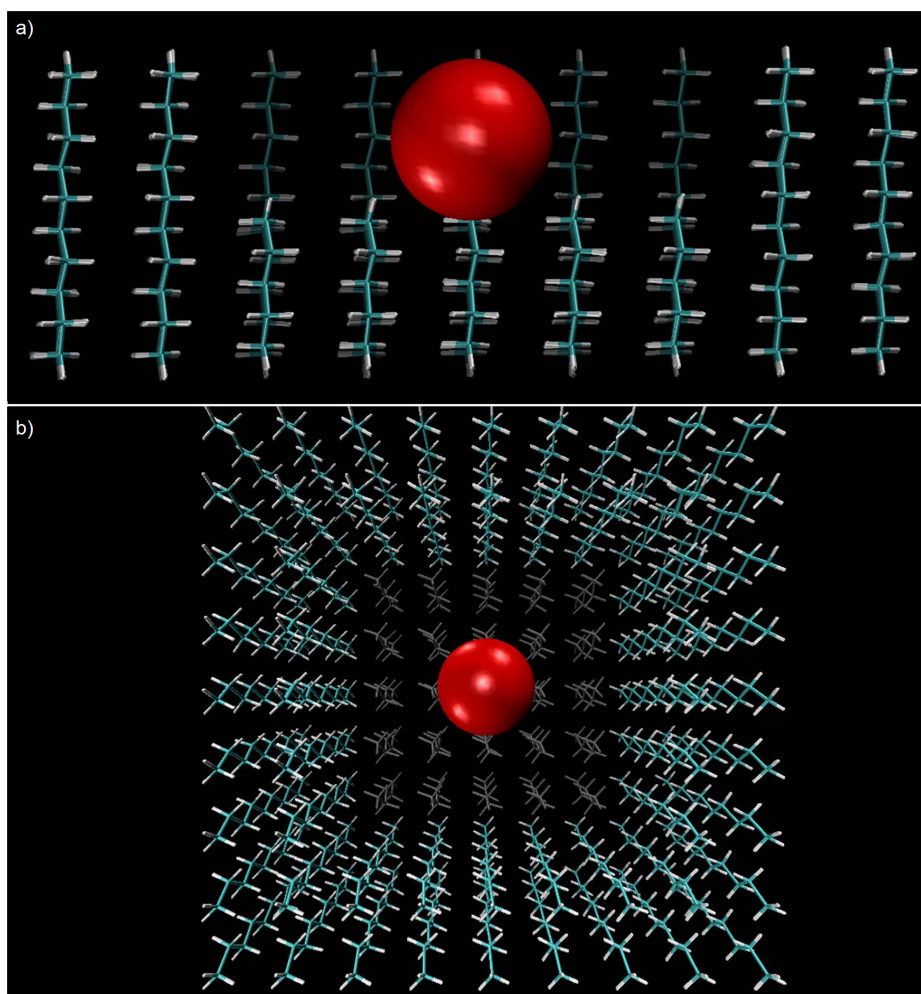


Figure 6: Idem to Fig. 5 but for the hole 25×5 . This hole was created by shortening all the central 25 chains in five units, as indicated by this nomenclature. a) side (cut) view. b) Top view. The central chains, which were shortened so as to generate the hole, are shown in light gray.

4. Conclusions

In this work we have studied the hydration properties of model surfaces as a function of the local geometry. Both for the graphitic surfaces (graphene and carbon nanotubes) and for alkane-like SAMs a significant orientational ordering of water molecules at the surface has been made evident. In both cases the H-O-H plane of the molecule tends to adopt an orientation almost

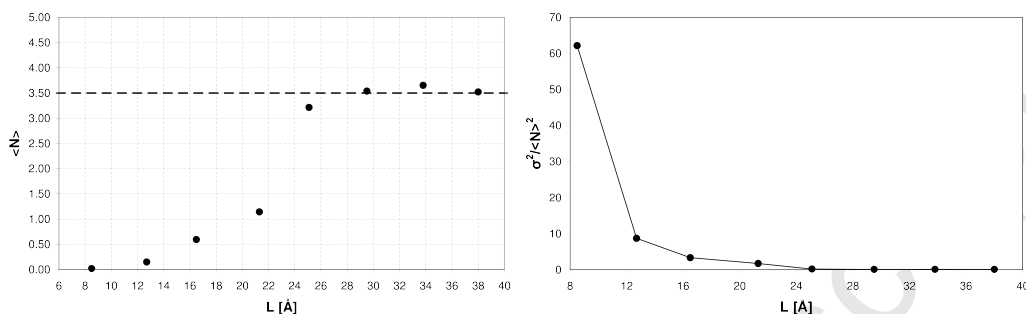


Figure 7: Left: Mean value of water molecules inside the observation volume for the holes as a function of hole width, L . The dashed line represent the value for the perfect monolayer (without hole). Right: Normalized density fluctuations for the holes as a function of hole width, L .

parallel to the surface, but for graphene the O-H bonds tend to point slightly outwards, forming an angle close to 70° with the surface normal, while for the SAM they point slightly inwards (to the surface), by forming an angle close to $100^\circ - 110^\circ$. Additionally, for convex graphitic-like surfaces we have demonstrated that, while water structuring depends on curvature, the hydrophobicity of the surface is practically curvature-independent as revealed by the water density fluctuations. However, for the case of pores carved in alkane-like surfaces, we have found that as curvature increases and the hole size enters the nanometric regime, the surface hydrophobicity increases significantly. Such a geometrically-induced dehydration might represent an interesting property for contexts like protein binding and materials design.

Acknowledgments

Financial support from MINCyT and CONICET is gratefully acknowledged. GAA, LMA and JARF are research fellows of CONICET. SRA and JMM thank CONICET for a fellowship. The authors wish to thank Prof. Pablo Debenedetti for enlightening discussions and for pointing out the interesting papers of Prof. S. Garde where the density fluctuations calculations were introduced.

- [1] D. M. Huang, D. Chandler, Proc. Natl. Acad. Sci. U.S.A. 97 (2000) 8324-8327.
- [2] X. Huang, C. J. Margulis and B. J. Berne, Proc. Natl. Acad. Sci. U.S.A. 100 (2003) 11953-11958.

- [3] A. Bizzarri and S. Cannistraro, *J. Phys. Chem. B* 106 (2002) 6617-6633.
- [4] D. Vitkup, D. Ringe, G. A. Petsko and M. Karplus, *Nat. Struct. Biol.* 7 (2000) 34-38.
- [5] N. Choudhury and B. Montgomery Pettitt, *J. Phys. Chem. B* 109 (2005) 6422-6429.
- [6] H. E. Stanley, P. Kumar, L. Xu, Z. Yan, M. G. Mazza, S. V. Buldyrev, S. -H. Chen and F. Mallamace, *Physica A* 386 (2007) 729-743.
- [7] N. Giovambattista, P. G. Debenedetti, C. F. Lopez, and P. J. Rossky, *Proc. Natl. Acad. Sci. U.S.A* 105 (2008) 2274-2279.
- [8] J. C. Rasaiah, S. Garde and G. Hummer, *Annu. Rev. Phys. Chem.* 59 (2008) 713-740.
- [9] J. Qvist, M. Davidovic, D. Hamelberg and B. Halle, *Proc. Natl. Acad. Sci. USA* 105 (2008) 6296-6301.
- [10] D.C. Malaspina, E.P. Schulz, L.M. Alarcón, M.A. Frechero and G.A. Appignanesi, *Eur. Phys. J. E* 32 (2010) 35-42.
- [11] E. Schulz, M. Frechero, G. Appignanesi and Ariel Fernández, *PLoS ONE* 5, e12844 (2010).
- [12] T. H. Rehm and C. Schmuck, *Chem. Soc. Rev.* 39 (2010) 35973611.
- [13] M. B. Sierra, S. R. Accordino, J. A. Rodríguez-Fris, M. A. Morini, G. A. Appignanesi and A. Fernández Stigliano, *Eur. Phys. J. E* 36 (2013) 62-69.
- [14] S. Vaitheeswaran, H. Yin, J.C. Rasaiah and G. Hummer, *Proc. Natl. Acad. Sci. USA* 101 (2004) 17002-17005.
- [15] E.P. Schulz, L.M. Alarcón and G.A. Appignanesi, *Eur. Phys. J. E* 34 (2011) 114-120.
- [16] G. Hummer, J.C. Rasaiah and J.P. Noworyta *Nature* 414 (2001) 188-190.
- [17] D. Takaiwa, I. Hatano, K. Koga and H. Tanaka, *Proc. Natl. Acad. Sci. USA* 105 (2008) 39-43.

- [18] M. Rana and A. Chandra, *J. Chem. Sci.* 119 (2007) 367-376.
- [19] K. Koga, G. T. Gao, H. Tanaka and X. C. Zeng, *Nature* 412 (2001) 802-805.
- [20] J. Wang, Y. Zhu, J. Zhou and X. Lu, *Phys. Chem. Chem. Phys.* 6 (2004) 829-835.
- [21] D. Bandyopadhyay and N. Choudhury, *J. Chem. Phys.* 136 (2012) 224505.
- [22] S. Pal, H. Weiss, H. Keller and F. Muller-Plathe, *Phys. Chem. Chem. Phys.* 7 (2005) 3191-3196.
- [23] S. N. Jamadagni, R. Godawat and S. Garde, *Annu. Rev. Chem. Biomol. Eng.* 2 (2011) 147-171.
- [24] H. Acharya, S. Vembanur, S. N. Jamadagni and S. Garde, *Faraday Discuss.* 146 (2010) 353-365.
- [25] W. L. Jorgensen, J. Chandrasekhar, J. D. Madura, R. W. Impey and M. L. Klein, *J. Chem. Phys.* 79 (1983) 926-935.
- [26] M. W. Mahoney and W. L. Jorgensen, *J. Chem. Phys.* 112 (2000) 8910-8922.
- [27] H. J. C. Berendsen, J. P. M. Postma, W. F. van Gunsteren, A. DiNola and J. R. Haak, *J. Chem. Phys.* 81 (1984) 3684-3690.
- [28] J-P. Hansen, I. R. McDonald, *Theory of Simple Liquids*, Third Edition, Academic Press (2006).
- [29] D. A. Case, T. A. Darden, I. T. E. Cheatham, C. L. Simmerling, J. Wang, R. E. Duke, R. Luo, K. M. Merz, D. A. Pearlman, M. Crowley, R. C. Walker, W. Zhang, B. Wang, S. Hayik, A. Roitberg, G. Seabra, K. F. Wong, F. Paesani, X. Wu, S. Brozell, V. Tsui, H. Gohlke, L. Yang, C. Tan, J. Mongan, V. Hornak, G. Cui, P. Beroza, D. H. Mathew, C. Schafmeister, W. S. Ross, and P. A. Kollman, AMBER9, University of California, San Francisco, CA, (2006).
- [30] T. Darden, D. York and L. Pedersen, *J. Chem. Phys.* 98 (1993) 10089-10092.

- [31] L.M. Alarcón, D.C. Malaspina, E.P. Schulz, M.A. Frechero, G.A. Appignanesi, *Chem. Phys.* 388 (2011) 4756.
- [32] Y. R. Shen and V. Ostroverkhov, *Chem. Rev.* 106 (2006) 1140-1154.
- [33] Y. Fan, X. Chen, L. Yang, P. S. Cremer and Y. Q. Gao, *J. Phys. Chem. B* 113 (2009) 11672-11679.
- [34] J. Gelman Constantin, A. Rodríguez Fris, G. A. Appignanesi, M. Carignano, I. Szleifer and H. Corti, *Eur. Phys. J. E* 34 (2011) 126-130.
- [35] E. Shiratani and M. Sasai, *J. Chem. Phys.* 104 (1996) 7671-7680.
- [36] E. Shiratani and M. Sasai, *J. Chem. Phys.* 108 (1998) 3264-3276.